



Original research article

Structural, optical and electrical properties of DC sputtered indium saving indium-tin oxide (ITO) thin films



Leandro Voisin^a, Makoto Ohtsuka^b, Svitlana Petrovska^{c,*}, Ruslan Sergiienko^d, Takashi Nakamura^b

^a AMTC, Advanced Mining Technology Center and DMin, Mining Engineering Department, University of Chile, Chile

^b Institute of Multidisciplinary Research for Advanced Materials (IMRAM), Tohoku University, Sendai 980-8577, Japan

^c National Academy of Science of Ukraine, Frantsevich Institute for Problems of Materials Science, 3 Krzhyzhanivsky Str., Kyiv 03680, Ukraine

^d National Academy of Science of Ukraine, Physico-Technological Institute of Metals and Alloys, 34/1 Vernadsky Ave., Kyiv 142 03680, Ukraine

ARTICLE INFO

Article history:

Received 8 June 2017

Received in revised form 7 December 2017

Accepted 7 December 2017

Keywords:

Indium tin oxide
Direct current sputtering
Electrical properties
Optical properties
Surface roughness

ABSTRACT

Amorphous indium tin oxide (ITO) thin films with reduced to 50 mass% indium oxide content were prepared by direct current (DC) sputtering of ITO target in mixed argon-oxygen atmosphere onto glass substrates preheated at 523 K. The films were subsequently heat-treated in air at different temperatures in the range of 523–923 K for 60 min. The use of oxygen during deposition resulted in highly transparent (>80%) in visible and infrared ranges of spectra films. It has been found from the electrical measurements that as-deposited films under optimum sputtering conditions at working gas flow rate of $Q(\text{Ar})/Q(\text{O}_2) = 50 \text{ sccm}/0.5 \text{ sccm}$ showed minimum volume resistivity of about $694 \mu\Omega\text{cm}$. As-deposited thin films obtained under the optimum condition showed amorphous structure. Improving of crystallisation has been observed with increasing heat treatment temperature. It has been found that DC sputtered films with decreasing amount of indium oxide have smooth surface in contrast to typical ITO (90 mass% indium oxide).

© 2017 Elsevier GmbH. All rights reserved.

1. Introduction

The major applications of the transparent conducting indium tin oxide (ITO) thin films are semiconducting window electrodes for solar cells and transparent conducting electrodes for liquid crystal displays (LCD's) [1–4]. Increasing demand for ITO thin films for industry provoked a significant increase in price of indium. Therefore in order to decrease the use of indium during the production of indium-tin-oxide films, a new target, which considers a smaller quantity of In_2O_3 in its composition and improves or maintains electrical and optical properties of typical ITO, is required to be developed. Details of the various deposition methods and characterization studies of indium saving ITO thin films have been reported [5–15]. Thirumoorthi et al. [7] have prepared ITO thin films with Sn concentration 0–30 mass% by jet nebulizer spray pyrolysis technique and found that film deposited at 20 mass% Sn showed the best optoelectronic properties. Similar result was obtained by Utsumi et al. [8] when depositing ITO thin films with 0–100 mass% SnO_2 by magnetron sputtering. Two peaks of carrier concentration at 5–10 atomic% of Sn and at 50 atomic% of Sn were revealed by Minami et al. [9]. ITO thin films with 50

* Corresponding author.

E-mail address: sw.piotrowska@gmail.com (S. Petrovska).

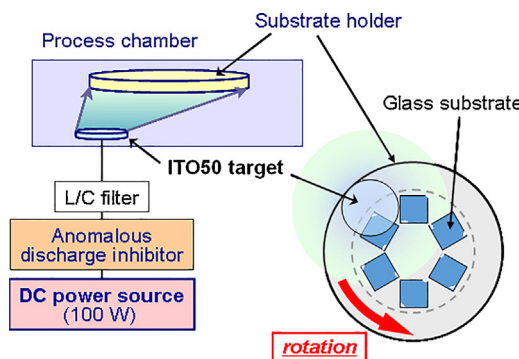


Fig. 1. Schematic diagram of the sputtering apparatus.

atomic% of Sn were obtained by Minami et al. [9–12] with low resistivity and high transmittance. In [9,11,12] it was shown that optical and electrical properties of ITO thin films with 50 atomic% of Sn are affected by both the substrate temperature and the oxygen content during deposition. O’Neil et al. [13] have described ITO thin films of composition $\text{In}_4\text{Sn}_3\text{O}_{12}$ obtained by pulsed laser deposition method. The structural, electrical and optical properties of these indium saving ITO thin films were considerably affected by the pressure of oxygen and substrate temperature. Li et al. [14] have studied the effects of oxygen flow rate and heat treatment on the optoelectronic properties of ITO thin films with ~50 mass% of SnO_2 deposited by RF magnetron sputtering method. However effect of heat treatment only at 300 °C was investigated. So there was no clear report on the effects of heat treatment on the ITO50 (50 mass% In_2O_3 -50 mass% SnO_2) films properties. A novelty of our work is to investigate the effect of heat treatment together with effects of Sn content and oxygen flow rate in a wide range of values on structural changes as well as related optical and electrical properties of the ITO50 films to have a clear understanding in order to use the films for suitable applications in various fields.

Sputtering is the most widely investigated technology available for ITO thin films large-scale production. In this work, we choose to deposit ITO50 thin films by DC sputtering method. It is well known that by increasing substrate temperature of ITO films [16,17], the structure of films can be changed and hence better optoelectrical properties can be obtained in comparison to those of thin films deposited onto unheated substrates. In this investigation ITO50 thin films with reduced to 50 mass% amount of indium oxide were sputtered onto glass substrates preheated at 523 K (PHS) under the rotation of the substrate holder in order to obtain a homogeneous deposition.

2. Experimental details

ITO50 (PHS) thin films were deposited onto glass substrates (Corning EAGLE 2000, surface: 50 mm × 50 mm, thickness: 0.7 mm) preheated at 523 K by DC sputtering method using a ceramic ITO50 target (Mitsui Mining & Smelting, 50 mass% In_2O_3 -50 mass% SnO_2). A schematic diagram of the sputtering apparatus (ULVAC, CS-200) used in the present study is shown in Fig. 1.

A resonance circuit (L/C) filter to eliminate ripple frequencies, an active arc killer (A2K) to prevent abnormal discharge, and a DC power source were used to sputter the ITO50 target. Process chamber was vacuumed at 10^{-5} Pa for its base pressure while total experimental pressures were resulted to be between 0.67 and 0.69 Pa. DC plasma power was kept at 100 W. Rotation speed for the substrate holder was set to 40 rpm. The argon flow rate $Q(\text{Ar})$ was kept constant at 50 sccm while oxygen flow rate $Q(\text{O}_2)$ changed in a wide range 0.1–1.0 sccm, and the deposition time was fixed at 30 min.

To measure thickness of sputtered thin films a very thin line of about 50 μm of width and 1 mm of length was removed with a laser (Laser X, LXSY-UV) in three positions, separated 1.5 mm to each other and located along the vertical line in a right part of the glass substrate. Depth of each line corresponding to film thickness was measured in each of those positions by using a scanning probe microscope (SPM, SII L-trace II), under dynamic force mode (DFM).

The deposited thin films were heat-treated in air at 523–923 K for 60 min and cooled to room temperature. Using the obtained thickness information, their optoelectrical properties were determined for both as-deposited (as-depo.) and heat-treated (HT) conditions. The measurements of volume resistivity ρ_V were carried out with a resistivity meter (Mitsubishi chemical analytech, Loresta GP Model MCP-T610) by using a 4-terminal method. Optical transmittance τ was measured into the 200–2600 nm range of wavelength using a Spectrophotometer (Hitachi High-Tech, U-4100).

Structural changes in the films caused by different heat-treated temperatures (523–923 K) were determined from their X-ray diffraction measurements using an X-ray diffractometer (Bruker, D2 phaser) with $\text{Cu}-\text{K}\alpha$ (wavelength: 0.15418 nm) radiation.

Surface analysis was taken for the as-depo. ITO50 thin films in comparison to ITO75 (75 mass% In_2O_3 -25 mass% SnO_2) and typical ITO90 (90 mass% In_2O_3 -10 mass% SnO_2) by using a scanning probe microscope (SPM, SII, L-trace II) under the DFM.

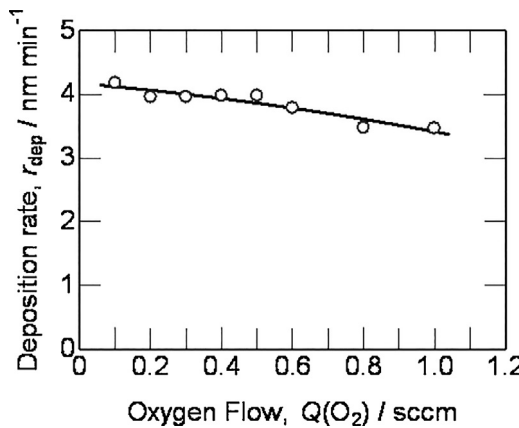


Fig. 2. ITO50 thin film deposition rate at different oxygen flow rates.

Table 1

Average thickness d_{ave} of ITO50 (PHS) thin films.

O ₂ flow rate, $Q(O_2)$ /sccm	0.1	0.2	0.3	0.4	0.5	0.6	0.8	1.0
Average thickness, d_{ave} /nm	125	119	119	119	119	114	104	104

Table 2

Volume resistivity of as-deposited ITO (PHS) thin films.

Sample	O ₂ flow rate, $Q(O_2)$ /sccm	Volume resistivity, $\rho_V/\mu\Omega\text{cm}$
ITO90 (PHS)	0.2	116
ITO75 (PHS)	0.3	318
ITO50 (PHS)	0.5	694

The ITO50 thin films to be investigated by transmission electron microscopy (TEM) were cut into cross-sectional specimens, which were ground, dimpled, and ion-milled to become electron transparent. The TEM characterization was carried out using a transmission electron microscope (Hitachi High Technology, H-9000NAR) operated at 300 kV.

3. Results and discussion

3.1. Deposition rate

ITO50 (PHS) thin films were deposited under different oxygen flow rates $Q(O_2) = 0.1\text{--}1.0$ sccm. Fig. 2 shows the relation between the deposition rate and the oxygen flow rate.

It was found that deposition rate continuously decreased from 4.2 to 3.5 nm/min when $Q(O_2)$ increased in the range from 0.1 to 1.0 sccm. Thickness of ITO50 (PHS) thin films listed in Table 1.

3.2. Electrical properties

Fig. 3 gives the volume resistivity ρ_V of ITO50 (PHS) thin films prepared at different oxygen flow rates. As the oxygen flow rate is increased ρ_V strongly decreased for both the as-depo. and heat-treated at HT523 films showing minimum at $Q(O_2) = 0.5$ and 0.8 sccm respectively. After that, the volume resistivity of the as-depo. film shows an increase as the oxygen flow rate is increased from 0.5 sccm to 1.0 sccm probably since vacancy-like oxygen defects were substituted by oxygen atoms and the additional oxygen atoms in the films function as carrier traps [18]. Tin in amorphous state is not efficiently activated and free carriers are contributed mainly by vacancy-like oxygen defects [19]. At the same time no significant changes in volume resistivity of thin films obtained at $Q(O_2) \geq 0.5$ sccm at $T_{HT} = 523$ K were observed (Fig. 3). However as the heat treatment temperature increases volume resistivity of the ITO50 (PHS) thin film sputtered under conditions that showed minimum resistivity for as-depo. state ($Q(O_2) = 0.5$ sccm) increases due to the filling of oxygen vacancies at high temperature [20]. ρ_V of thin film deposited at $Q(O_2) = 0.8$ sccm showed rapid decrease at HT523, HT723 and HT923. The minimum value for ρ_V of $665 \mu\Omega\text{ cm}$ was obtained from the HT523 ITO50 (PHS) film deposited at $Q(O_2) = 0.8$ sccm. This value is higher in comparison to that of ρ_V obtained from the ITO75 (PHS) deposited at $Q(O_2) = 0.3$ sccm and ITO90 (PHS) as-depo. films sputtered under $Q(O_2) = 0.2$ sccm, respectively (Table 2). Such increase of volume resistivity with increasing of tin oxide amount was observed since the tin ion, which is surrounded only by In₂O₃ at a low SnO₂ content in ITO90 can behave as a donor whereas in an overdoped state the excess of Sn leads to suppression in its donor ability [21]. This result is also correlated with the loss of crystallinity in ITO films for higher than optimum dopant levels [21].

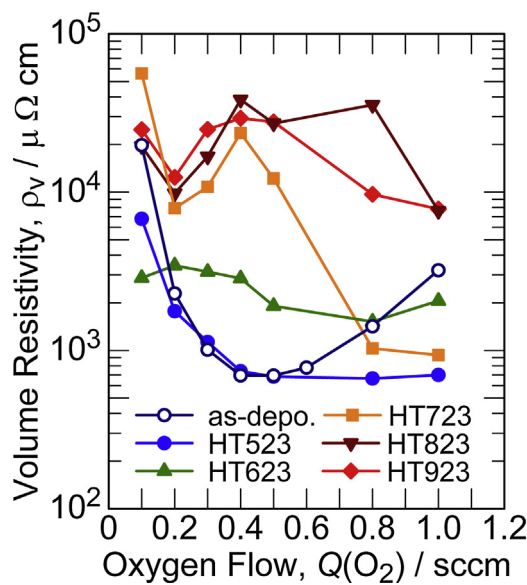


Fig. 3. Effects of oxygen flow rate and heat treatment temperature on the volume resistivity of ITO50 (PHS) thin films.

Table 3

Mobility and carrier density of as-deposited ITO (PHS) thin films with 150 nm thickness.

Sample	O ₂ flow rate, Q(O ₂)/sccm	Mobility, μ/cm ² V ⁻¹ s ⁻¹	Carrier density, n/cm ⁻³
ITO90 (PHS)	0.2	36	1.62 × 10 ²¹
ITO50 (PHS)	0.5	40	1.57 × 10 ²⁰

As is reported in Table 3, carrier density of ITO50 (PHS) is one order lower than that of ITO90 (PHS), whereas mobility of ITO50 (PHS) is slightly higher as compared to ITO90 (PHS) due to absence of structural discontinuities in amorphous state. The same tendency was observed in other studies [5,6].

At the same time ρ_V data for as-deposited ITO50 (PHS) are promising in comparison to that of ITO50 thin films deposited on unheated substrates (UHS). The later showed relatively low volume resistivity of 2990 $\mu\Omega\text{cm}$ only after HT at high temperatures (923 K).

3.3. Optical properties

Transmittance spectral measurements for ITO50 (PHS) thin films sputtered at different oxygen flow rates are shown in Fig. 4a.

Fig. 4a shows that the transmittance in visible range noticeably increases with increasing oxygen flow rate up to 0.5 sccm and keeps almost the same value under $Q(O_2) > 0.5$ sccm showing $\tau > 85\%$. Such increase can be connected with decreasing of film thickness when oxygen flow rate increases. τ in infrared (IR) region increases with increasing oxygen flow rate except the sample obtained at $Q(O_2) = 0.2$ sccm. It can be explained by an increase of the amount of free electrons with decreasing $Q(O_2)$, because the electrons are from oxygen vacancies in the film [22].

τ curves for as-depo. and heat-treated ITO50 (PHS) thin films sputtered under the condition of $Q(O_2) = 0.5$ sccm at which the best electrical properties were observed are shown in Fig. 4b. Optical transmittance is higher than 93% at $\lambda = 550$ nm and does not change with increasing heat treatment temperature.

Fig. 4c shows that transmittance of ITO50 (PHS) at $\lambda = 550$ nm is higher than that of ITO75 and ITO90 and kept high in the near infrared and infrared regions of the spectrum in contrast to that of ITO75 (PHS) and ITO90 (PHS) thin films, which are opaque in this wavelength range. Higher transmittance in the IR part of the spectrum is optional for example in new transparent electrodes for QD-LED.

For small thicknesses ITO90 thin films are transparent in IR, and at a thickness of 150 nm in other works [3,23] the transparency is much higher (>50%) than transmittance of ITO90 presented in our work (less than 20%). It can be explained by higher carrier concentration of ITO90 thin film in our work ($1.62 \times 10^{21} \text{ cm}^{-3}$) in comparison with lower carrier concentration ($1.12 \times 10^{20} \text{ cm}^{-3}$, $5.5 \times 10^{20} \text{ cm}^{-3}$) observed by other authors [14,23]. Such a difference in the carrier concentration can be explained by different conditions for the deposition of films.

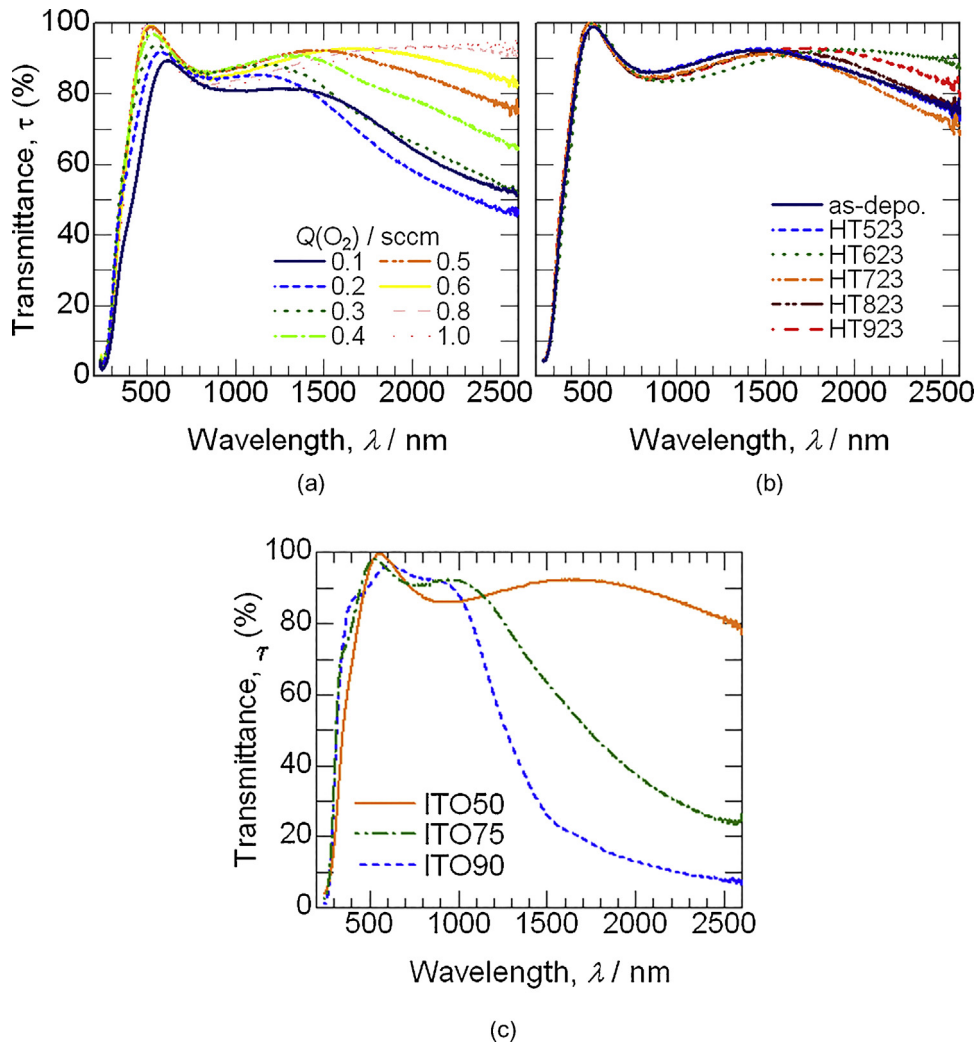


Fig. 4. Effects of oxygen flow rates (a) and heat treatment temperature (b) on the transmittance of ITO50 (PHS) thin films and comparison of τ curves of as-depo. ITO50 (PHS) obtained at $Q(Ar)/Q(O_2)=50$ sccm/0.5 sccm, as-depo. ITO75 (PHS) sputtered at $Q(Ar)/Q(O_2)=50$ sccm/0.3 sccm and as-depo. ITO90 (PHS) obtained at $Q(O_2)=50$ sccm/0.2 sccm (c).

3.4. Structural characterization

XRD patterns of as-depo. and heat-treated ITO50 (PHS) thin films sputtered under optimum condition $Q(O_2)=0.5$ sccm are shown in Fig. 5a. As-depo. film may be regarded as amorphous since no X-ray diffraction peaks were revealed. The hump between $2\theta=20^\circ$ and 30° is owing to the background of the glass substrates. As can be seen from Fig. 5a heat treatment at 523–723 K did not improve crystallinity of ITO50 (PHS) samples sputtered at $Q(O_2)=0.5$ sccm. At the heat treatment temperature of 823 K the prominent diffraction peaks appeared showing polycrystalline structure corresponding to $In_4Sn_3O_{12}$ [24]. In opposite to amorphous as-depo. ITO50 (PHS) thin film the un-annealed ITO75 (PHS) and ITO90 (PHS) film are crystalline in nature with dominant (222) plane (Fig. 5b). The analysis of XRD patterns of ITO75 (PHS), ITO90 (PHS) films reveals that the peak positions of (211), (222), (400), (431), (440), and (622) planes agree fairly well with JCPDS card No. 71-2194 for cubic bixbyite structure. Results of XRD analysis were summarized in Table 4. The X-ray diffraction profile of $In_4Sn_3O_{12}$ shows a clear difference from that of In_2O_3 , in particular the standard diffraction profile of $In_4Sn_3O_{12}$ shows first relatively intensive peak at 18.744° , but indium oxide In_2O_3 has first peak from reflection (211) at 21.497° . The experimental XRD profile of crystallized ITO50 (PHS) $Q(Ar)/Q(O_2)=50$ sccm/0.5 sccm film showed fist peak at 18.850° .

Fig. 6 shows TEM images of the cross-section of the as-deposited ITO50 (PHS) thin film with 150 nm thickness. From these results it is clear that ITO50 thin film consists of two regions. The first one near glass substrate possesses most likely to be amorphous structure. The first region is thinner and may be as thick as about 30 nm. The second region consists of the individual columns, which are single crystals.

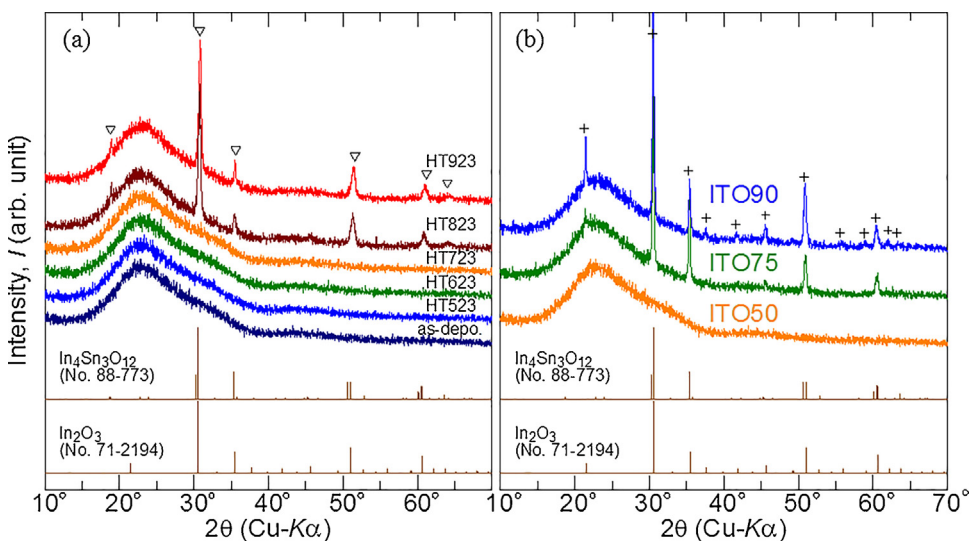


Fig. 5. (a) XRD results for ITO50 (PHS) thin films deposited at $Q(\text{Ar})/Q(\text{O}_2) = 50 \text{ sccm}/0.5 \text{ sccm}$; (b) XRD pattern of as-deposited ITO50 (PHS) sputtered at $Q(\text{Ar})/Q(\text{O}_2) = 50 \text{ sccm}/0.5 \text{ sccm}$, ITO75 (PHS) deposited at $Q(\text{Ar})/Q(\text{O}_2) = 50 \text{ sccm}/0.3 \text{ sccm}$ and ITO90 (PHS) film obtained at $Q(\text{Ar})/Q(\text{O}_2) = 50 \text{ sccm}/0.2 \text{ sccm}$.

Table 4

X-ray diffraction data of as-deposited ITO90 (PHS) [$Q(\text{O}_2) = 0.2 \text{ sccm}$] and ITO75 (PHS) [$Q(\text{O}_2) = 0.3 \text{ sccm}$] films and ITO50 (PHS) film [$Q(\text{O}_2) = 0.5 \text{ sccm}$] heat-treated at 923 K with the main standard data of In₄Sn₃O₁₂ [24] and In₂O₃ [25].

Standard data (JCPDF)											
In ₂ O ₃ (No. 71-2194)			In ₄ Sn ₃ O ₁₂ (No. 88-773)			ITO90 (PHS) as-depo.		ITO75 (PHS) as-depo.		ITO50 (PHS) HT923	
hkl	$2\theta / ^\circ$	I / I_0	hkl	$2\theta / ^\circ$	I / I_0	$2\theta / ^\circ$	I / I_0	$2\theta / ^\circ$	I / I_0	$2\theta / ^\circ$	I / I_0
211	21.497	12	110	18.744	3	21.499	21	21.431	13	18.850	8
			012	22.805	3						
			021	23.913	3						
			003	30.243	34						
222	30.586	100	12-1	30.557	100	30.542	100	30.551	100	30.866	100
			21-2	35.338	39						
			11-3	35.820	3						
411	37.693	5				37.675	4	45.613	5	51.530	22
332	41.847	4				41.807	3	50.943	2	59.043	10
431	45.689	8	303	45.188	3	45.600	8	51.039	22	60.600	10
			12-4	50.634	24						
			14-3	60.487	18						
440	51.025	33	140	51.043	24	50.943	27	63.382	4	64.122	4
			32-2	52.872	4						
611	55.985	4				55.878	1	62.161	3	66.127	12
541	59.134	4	502, 21-5	60.121	10	59.043	2	63.382	4	66.127	12
			14-3	60.487	18						
622	60.669	23	42-1	60.669	18	60.600	10	60.693	11	61.127	12
631	62.182	5				62.161	3	63.382	4	66.127	12
444	63.675	4	24-2	63.610	7	63.382	4	66.127	12	66.127	12
			15-1	64.099	2						

It was performed the detailed investigation of the film in two regions – near the glass substrate and region of individual columns using Fast Fourier Transformation (FFT). The region near the glass substrate (Fig. 7a) is amorphous and that is confirmed by the diffused ring on the FFT image (Fig. 7c). The FFT analysis of high resolution image from the single crystal columns (Fig. 7b) showed the diffraction spots from crystal planes with the lattice d -spacings of about 0.29 and 0.18 nm. Thus, TEM investigations confirmed the XRD analysis and both methods showed a low crystallinity of as-deposited ITO50 (PHS) films.

Surface studies were aimed at examining the possible correlation between the surface morphology and the optoelectrical properties of thin films under investigation. Fig. 8 shows the surface morphology of ITO50 (PHS) thin films showed the lowest volume resistivity at $Q(\text{O}_2) = 0.5 \text{ sccm}$ comparing to ITO75 (PHS) and ITO90 (PHS) sputtered under optimum conditions $Q(\text{O}_2) = 0.3 \text{ sccm}$ and $Q(\text{O}_2) = 0.2 \text{ sccm}$, respectively.

Root mean square height (S_q) and arithmetical mean height (S_a) of as-depo. ITO (PHS) thin films are presented in Table 5.

According to the DFM results shown in Table 5, amorphous ITO50 (PHS) thin film sputtered at $Q(\text{O}_2) = 0.5 \text{ sccm}$ showed the lowest roughness. So surface roughness of ITO (PHS) thin films decreased with decreasing In_2O_3 amount in target similar

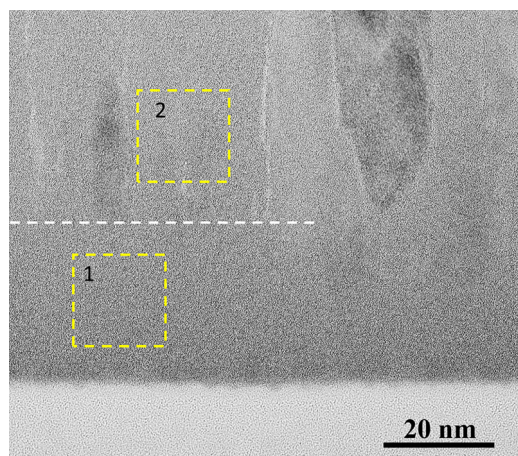


Fig. 6. Bright-field TEM image of the cross-sectional ITO50 (PHS) thin film deposited on the glass substrate under $Q(\text{Ar})/Q(\text{O}_2) = 50 \text{ sccm}/0.3 \text{ sccm}$. The dashed straight line shows approximate boundary between two regions.

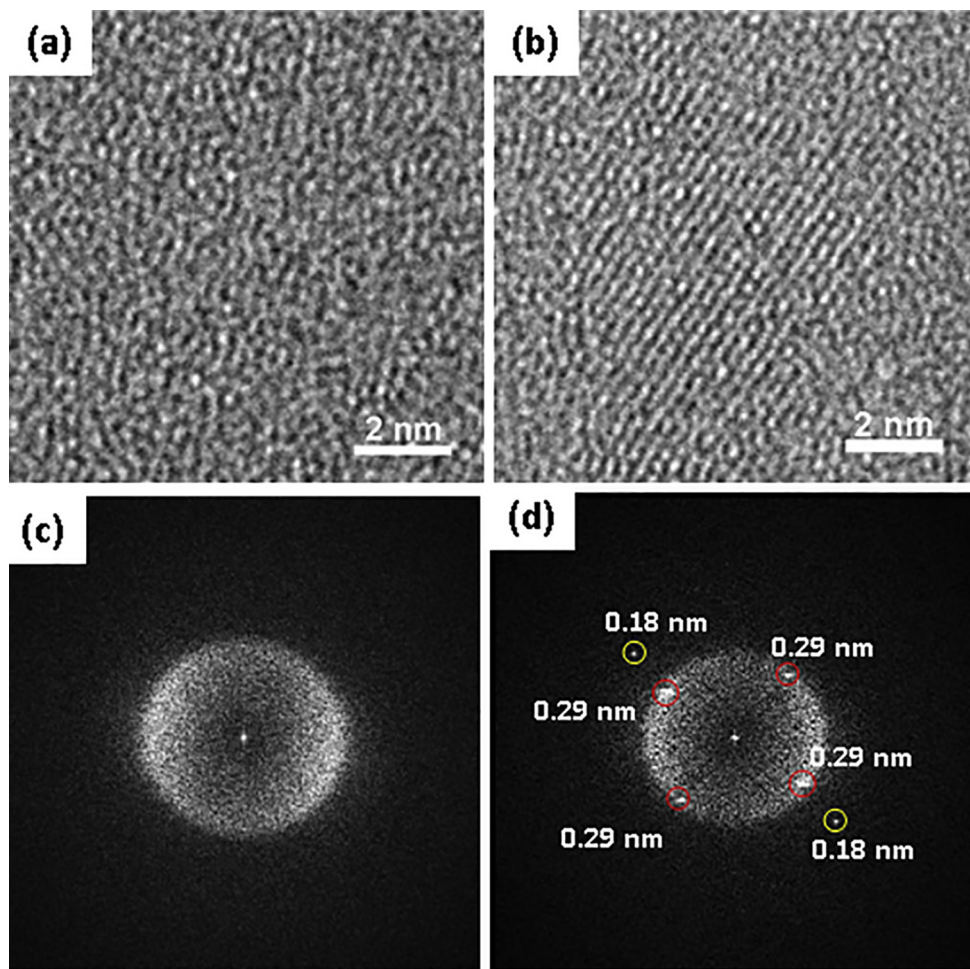


Fig. 7. (a) and (b) The enlarged high resolution images of the areas surrounded by rectangles 1 and 2 in Fig. 6, respectively; (c) and (d) corresponding digital diffractograms computed by Fast Fourier Transformation of the images shown in (a) and (b), respectively.

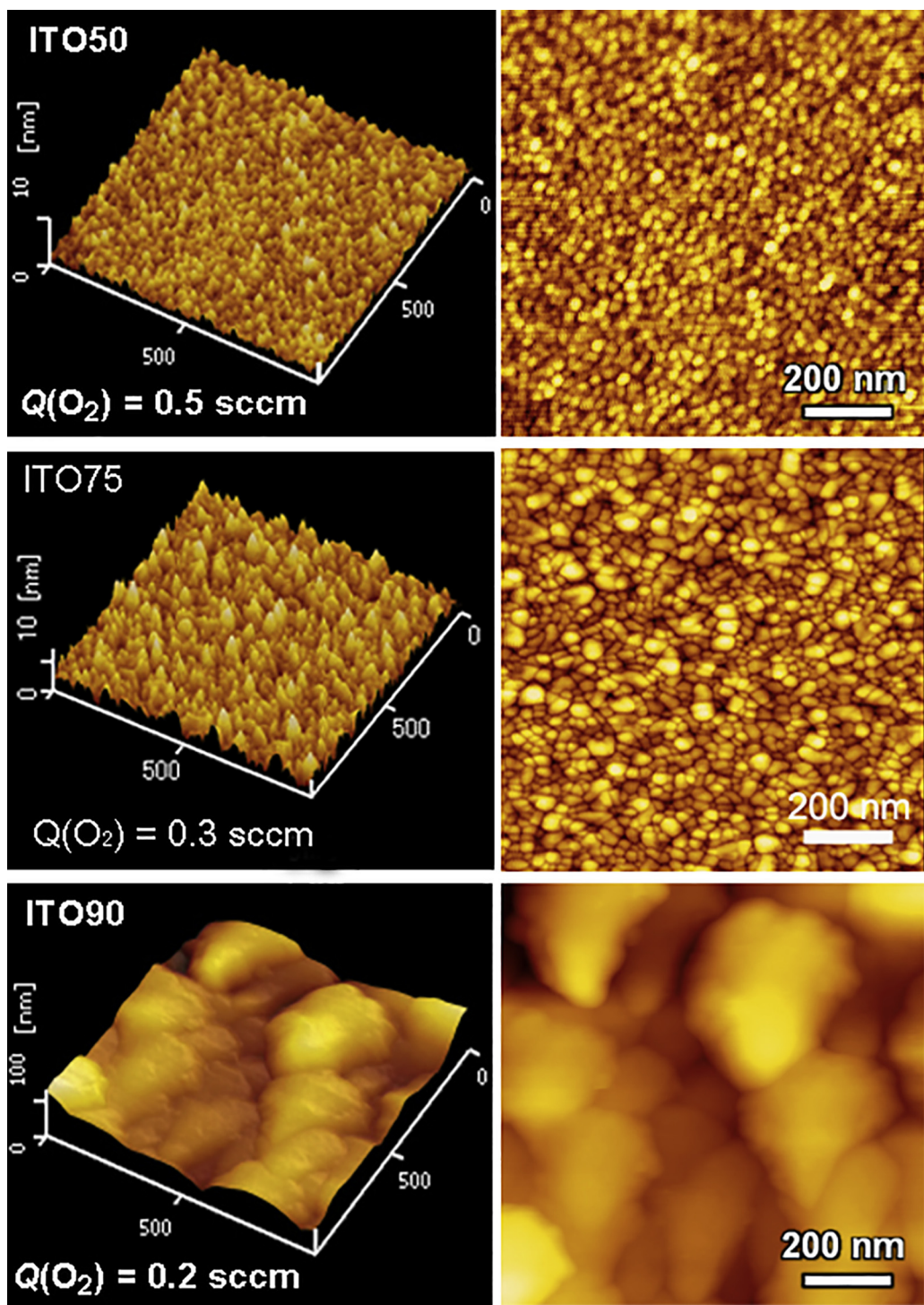


Fig. 8. Surface analysis results for as-depo. ITO50 (PHS) thin films deposited under $Q(\text{Ar})/Q(\text{O}_2) = 50 \text{ sccm}/0.5 \text{ sccm}$ in comparison to ITO75 (PHS) $Q(\text{Ar})/Q(\text{O}_2) = 50 \text{ sccm}/0.3 \text{ sccm}$ and ITO90(PHS) $Q(\text{Ar})/Q(\text{O}_2) = 50 \text{ sccm}/0.2 \text{ sccm}$.

to results obtained in [7] for ITO with Sn concentration 0–30 wt%. Due to smooth uniform surface of ITO50 (PHS) thin films are highly transparent.

Table 5

Root mean square height (S_q) and arithmetical mean height (S_a) of as-deposited ITO (PHS) thin films.

Sample	O ₂ flow rate, Q(O ₂)/sccm	Root mean square height, S_q /nm	Arithmetical mean height, S_a /nm
ITO90	0.2	15.7	12.8
ITO75	0.3	1.83	1.44
ITO50	0.5	0.61	0.49

4. Summary

Indium saving ITO thin films have been deposited onto glass substrates preheated at 523 K by DC sputtering at different oxygen flow rates and subsequently heat treated. In order to reduce indium usage in ITO films, an amount of indium oxide in the target was decreased from 90 to 50 mass%. The deposition rate shows a clear decrease with increasing of oxygen flow rate. The crystallinity of ITO50 (PHS) films was dominantly affected by heat treatment temperature. The electrical properties of ITO50 (PHS) were improved compared to the films deposited onto unheated substrates. Minimum volume resistivity of 694 $\mu\Omega\text{cm}$ was obtained for the as-depo. ITO50 film using a mixture of argon and oxygen $Q(\text{Ar})/Q(\text{O}_2) = 50 \text{ sccm}/0.5 \text{ sccm}$ as sputtering gas. The resistivity of the films was found to be depended on the evolution of the structure, the oxygen content and the heat treatment temperature. The transmittance values were higher than 80% at $\lambda = 450\text{--}2600 \text{ nm}$ for films obtained at optimum sputtering conditions. ITO50 (PHS) thin films were obtained with very smooth surface in contrast to typical ITO. Surface roughness of ITO (PHS) thin films decreased to $S_a = 0.49 \text{ nm}$, $S_q = 0.61 \text{ nm}$ with decreasing amount of In_2O_3 in target from 90 to 50 mass%. Thus the indium content in ITO thin films could be reduced as high as 50 mass% making it possible to obtain thin films with suitable optoelectronic properties.

Acknowledgment

The present research was supported by New Energy and Industrial Technology Development Organization (NEDO), Japan.

References

- [1] J. Hotovy, J. Hüpkes, W. Böttler, E. Marins, L. Spiess, T. Kups, V. Smirnov, I. Hotovy, J. Kováč, Sputtered ITO for application in thin-film silicon solar cells: relationship between structural and electrical properties, *Appl. Surf. Sci.* 269 (2013) 81–87.
- [2] D.-W. Kang, A. Chowdhury, P. Sichanugrist, Y. Abe, H. Konishi, Y. Tsuda, T. Shinagawa, H. Tokioka, H. Fuchigami, M. Konagai, Highly transparent $\text{Zn}_{1-x}\text{Mg}_x\text{O}$ /ITO multilayer for window of thin film solar cells, *Curr. Appl. Phys.* 15 (2015) 1022–1026.
- [3] K.P. Sibin, N. Swain, P. Chowdhury, A. Dey, N. Sridhara, H.D. Shashikala, A.K. Sharma, H.C. Barshilia, Optical and electrical properties of ITO thin films sputtered on flexible FEP substrate as passive thermal control system for space applications, *Sol. Energy Mater. Sol. Cells* 145 (2016) 314–322.
- [4] B. Hirschmann, G. Oreski, G. Pinter, Thermo-mechanical characterization of fluoropolymer films for concentrated solar thermal applications, *Sol. Energy Mater. Sol. Cells* 130 (2014) 615–622.
- [5] P.K. Biswas, A. De, K. Ortner, S. Korder, Study of sol–gel-derived high tin content indium tin oxide (ITO) films on silica-coated soda lime silica glass, *Mater. Lett.* 58 (2004) 1540–1545.
- [6] P.K. Biswas, A. De, N.C. Pramanika, P.K. Chakraborty, K. Ortner, V. Hock, S. Korder, Effects of tin on IR reflectivity, thermal emissivity, Hall mobility and plasma wavelength of sol–gel indium tin oxide films on glass, *Mater. Lett.* 57 (2003) 2326–2332.
- [7] M. Thirumoorthi, J. Thomas Joseph Prakash, Structure, optical and electrical properties of indium tin oxide ultrathin films prepared by jet nebulizer spray pyrolysis technique, *J. Asian Ceram. Soc.* 4 (2016) 124–132.
- [8] K. Utsumi, H. Iigusa, R. Tokumaru, P.K. Song, Y. Shigesato, Study on $\text{In}_2\text{O}_3\text{--SnO}_2$ transparent and conductive films prepared by d.c. sputtering using high density ceramic targets, *Thin Solid Films* 445 (2003) 229–234.
- [9] T. Minami, Y. Takeda, S. Takata, T. Kakumu, Preparation of transparent conducting $\text{In}_4\text{Sn}_3\text{O}_{12}$ thin films by DC magnetron sputtering, *Thin Solid Films* 308–309 (1997) 13–18.
- [10] T. Minami, T. Miyata, T. Yamamoto, Work function of transparent conducting multicomponent oxide thin films prepared by magnetron sputtering, *Surf. Coat. Technol.* 108–109 (1998) 583–587.
- [11] T. Minami, T. Kakumu, K. Shimokawa, S. Takata, New transparent conducting $\text{ZnO}\text{--In O}\text{--SnO}$ thin films prepared by magnetron sputtering, *Thin Solid Films* 317 (1998) 318–321.
- [12] T. Minami, Transparent and conductive multicomponent oxide films prepared by magnetron sputtering, *J. Vac. Sci. Technol. A* 17 (1999) 1765–1772.
- [13] D.H. O’Neil, V.L. Kuznetsov, R.M.J. Jacobs, M.O. Jones, P.P. Edwards, Structural, optical and electrical properties of $\text{In}_4\text{Sn}_3\text{O}_{12}$ films prepared by pulsed laser deposition, *Mater. Chem. Phys.* 123 (2010) 152–159.
- [14] S. Li, X. Qiao, J. Chen, Effects of oxygen flow on the properties of indium tin oxide films, *Mater. Chem. Phys.* 98 (2006) 144–147.
- [15] M. Epifani, R. Diaz, J. Arbiol, P. Siciliano, J.R. Morante, Solution synthesis of thin films in the $\text{SnO}_2\text{--In}_2\text{O}_3$ system: A case study of the mixing of sol–gel and metal-organic solution processes, *Chem. Mater.* 18 (2006) 840–846.
- [16] L. Bo, C. Shuying, Properties of indium tin oxide films deposited by RF magnetron sputtering at various substrate temperatures, *Micro Nano Lett.* 7 (2012) 835–837.
- [17] J. Xu, Y. Yuan, F. Wang, K. Zhang, Influence of substrate temperature on properties of indium tin oxide thin films prepared by DC magnetron sputtering, *ECS Trans.* 44 (2012) 1311–1316.
- [18] K.-H. Kim, The preparation of indium tin oxide films as a function of oxygen gas flow rate by a facing target sputtering system, *J. Ceram. Process. Res.* 8 (2007) 19–21.
- [19] D.C. Pain, H.-Y. Yeom, B. Yaglioglu, Transparent conducting materials and technology, in: G.P. Crawford (Ed.), *Flexible Flat Panel Displays*, Wiley, West Sussex, 2005, pp. 79–98.
- [20] H.A. Mohamed, The effect of annealing and ZnO dopant on the optoelectronic properties of ITO thin films, *J. Phys. D Appl. Phys.* 40 (2007) 4234–4240.
- [21] H. Kim, C.M. Gilmore, A. Piqué, J.S. Horwitz, H. Mattoussi, H. Murata, Z.H. Kafafi, D.B. Chrisey, Electrical, optical, and structural properties of indium-tin-oxide thin films for organic light-emitting devices, *J. Appl. Phys.* 86 (1999) 6451–6461.
- [22] M. Bender, W. Seelig, C. Daube, H. Frankenberaer, B. Ocker, J. Stollenwerk, Dependence of oxygen flow on optical and electrical properties of DC-magnetron sputtered ITO films, *Thin Solid Films* 326 (1998) 72–77.

- [23] M.D. Benoy, E.M. Mohammed, M. Suresh Babu, P.J. Binu, B. Pradeep, Thickness dependence of the properties of indium tin oxide (ITO) FILMS prepared by activated reactive evaporation, *Braz. J. Phys.* 39 (2009) 629–632.
- [24] N. Nadaud, M. Nanot, J. Jove, T. Roisnel, A structural study of tin-doped indium oxide (ITO) ceramics using ^{119}Sn Mössbauer spectroscopy and neutron diffraction, *Key Eng. Mater.* 132 (1997) 1373–1376.
- [25] M. Marezio, Refinement of the crystal structure of In_2O_3 at two wavelengths, *Acta Cryst.* 20 (1966) 723–728.